Pyridyl- and Picolinic Acid Substituted Zinc(II) Phthalocyanines for Dye-Sensitized Solar Cells

Juan Suanzes Pita,[a] Maxence Urbani,[a, b, c] Giovanni Bottari,[a, c, d] Mine Ince,[b] Sangeeta Amit Kumar,[b] Aravind Kumar Chandiran,[b] Jun-Ho Yum,[b] Michael Grätzel,[b] Mohammad Khaja Nazeeruddin,*[e] and Tomas Torres*[a, c, d]

A series of tri-tert-butyl zinc(II) phthalocyanines (Pcs) substituted with pyridyl, carboxyl, or picolinic acid anchoring groups on the periphery were prepared. Photovoltaic (PV) studies on these dyes were carried out revealing some interesting features. In the case of the pyridyl-substituted Pcs, the PV properties were found to depend strongly on the the pyridyl substitution pattern (meta or para) and the number of pyridyl units at the macrocycle's periphery (one or two). For these four pyridyl-substituted Pcs, higher photovoltaic efficiencies were obtained for 1) the para- versus the meta-substituted Pcs, and 2) the mono- versus the bis-functionalized dyes. In order to improve the poor adsorption of the pyridyl-substituted Pcs onto TiO2, a new dye was tested bearing a picolinic acid unit. This moiety combines a carboxylic acid function, as a strong anchoring group for binding to TiO2, with an electron-withdrawing nitrogen atom for better electron injection into the semiconductor's conduction band. For this latter system, an improvement in the PV efficiency up to 2.1% was obtained.

In the field of dye-sensitized solar cells (DSSCs), porphyrins (Pors)[1] and phthalocyanines (Pcs)[2,3] have attracted special attention due to their high extinction coefficients and chemical and thermal robustness. Until recently, the great majority of sensitizers used in DSSCs have been endowed mostly with carboxylic acid or cyanoacrylic acid moieties acting both as electron-acceptor units and anchoring groups for attachment to TiO2 surfaces. The search for novel anchoring groups that bind better than conventional carboxylic acids to the TiO2 surface is a topic of intense research.[4,5] In 2011 Ooyama et al. reported the use of pyridyl units as electron-withdrawing anchoring groups in donor–π-conjugated–acceptor dyes (D-π-A). This efficient alternative to the traditional approach allows good electronic communication between the dye and TiO2, and therefore efficient electron injection.[6] In this case, coordinate bonds form between the pyridyl ring and the Lewis acid sites of TiO2 surface, rather than the ester linkages with the Brønsted acid sites of TiO2 surface typically observed for carboxylic acid sensitizers. Later on, this concept was applied to Pors[7–9] and more recently to Pcs.[10,11] Despite their great potential, very few examples of systems combining N-heterocycles and carboxylic acid moieties have been described.[11,12] For instance, Delcamp et al. reported various acceptor motifs based on N-heterocycles that offer the possibility to tune the electron-withdrawing character, spectral absorption, and the excited-state oxidation potential of the dye with minimal effect on the ground-state oxidation potential.[12] These effects have a large impact on the charge separation and charge injection. Recently, Mai et al. reported the use of 2-carboxypyridine as an efficient and stable anchoring group for a push–pull Por.[11] The device made from this dye showed better photovoltaic (PV) performances and long-term stability than the carboxyl- and pyridyl-based analogues.

Herein, we have investigated the PV properties of a series of tri-tert-butyl zinc(II) phthalocyanines bearing pyridyl, carboxyl, or picolinic acid moieties as anchoring groups to TiO2 (Figure 1). In the case of the pyridyl-substituted Pcs, a strong dependence of the device performance on the pyridyl substitution pattern (meta or para) and the number of pyridyl units attached on the Pc periphery (one or two) was found. However, an important limitation of these pyridyl-substituted ZnIIPcs was their low adsorption on TiO2, which ultimately resulted in

[a] J. Suanzes Pita, Dr. M. Urbani, Dr. G. Bottari, Prof. Dr. T. Torres
Departamento de Química Orgánica
Universidad Autónoma de Madrid
28049 Madrid (Spain)
E-mail: tomas.torres@uam.es

[b] Dr. M. Urbani, Dr. M. Ince, S. A. Kumar, A. K. Chandiran, J.-H. Yum, Prof. M. Grätzel
Laboratory of Photonics and Interfaces
Institute of Chemical Sciences and Engineering
Swiss Federal Institute of Technology (EPFL)
Station 6, 1015 Lausanne (Switzerland)

[c] Dr. M. Urbani, Dr. G. Bottari, Prof. Dr. T. Torres
IMDEA-Nanociencia
Campus de Cantoblanco
28049 Madrid (Spain)

[d] Dr. G. Bottari, Prof. Dr. T. Torres
Institute for Advanced Research in Chemical Sciences (IAdChem)
Universidad Autónoma de Madrid, 28049 Madrid (Spain)

[e] Prof. Dr. M. K. Nazeeruddin
Group for Molecular Engineering of Functional Materials
Institute of Chemical Sciences and Engineering
School of Basic Sciences, Swiss Federal Institute of Technology (EPFL)
1951 Sion (Switzerland)
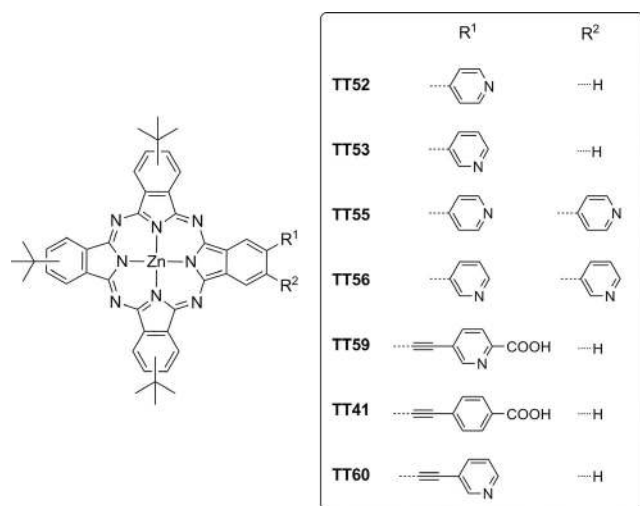E-mail: mdkhaja.nazeeruddin@epfl.ch

Figure 1. Molecular structures of Zn^{II}Pcs studied in this work.

moderate power conversion efficiencies (PCEs). In order to mitigate this problem, a Pc was prepared with a picolinic acid unit on the periphery, an anchoring moiety that combines a carboxylic acid function, known to strongly bind to the TiO$_2$, with an electron-withdrawing nitrogen atom for better electron injection into the semiconductor's conduction band.

The detailed synthesis and characterization of the prepared pyridyl-, carboxyl-, and picolinic acid substituted Pcs can be found in the Supporting Information. We first investigated the DSSC performances of mono- (**TT52** and **TT53**) and di- (**TT54** and **TT55**) pyridyl-substituted Zn^{II}Pcs adsorbed on a [6+3] µm thick film of TiO$_2$ and used an iodine-based electrolyte typically employed for Pc sensitizers[13] (electrolyte A; Table 1). The dye solutions were prepared in THF at a concentration of 0.1 mM with 10 mM of chenodeoxycholic acid (CHENO) as co-adsorbent. A large excess of co-adsorbent with respect to the Zn^{II}Pc (100-fold) is typically used for this kind of sensitizer in order to

Table 1. PV data of the devices[a] made with dyes **TT52**, **TT53**, **TT55**, and **TT56** on [6+3] µm[b] thick TiO$_2$ films using the iodine-based liquid electrolyte A,[c] under simulated full sun illumination (AM1.5G) and with an active area of 0.159 cm^{-2}.
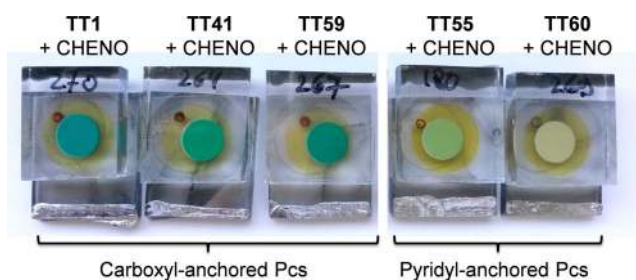
Dye/CHENO[d]	V_{OC} [mV]	J_{SC} [mA cm^{-2}]	FF [%]	P_{in} [mW cm^{-2}]	η [%]
TT52+CHENO	567	3.44	68.0	100.1	1.3
TT53+CHENO	555	1.08	73.6	100.6	0.44
TT55+CHENO	568	2.01	77.3	99.4	0.89
TT56+CHENO	493	0.301	74.3	96.5	0.11

[a] Two or three devices of equal quality were made for each dye; the values obtained for the best cell are presented in each case. [b] The TiO$_2$ films have a total thickness of 9 µm consisting of a 6 µm thick TiO$_2$ active layer and an additional 3 µm thick scattering layer. [c] Electrolyte A: 0.025 M LiI, 0.9 M 1,3-dimethylimidazolium iodide (DMII), 0.28 M 4-tert-butyl pyridine (TBP), 0.04 M I$_2$, and 0.05 M guanidinium thiocyanate (GuNCS) in AcCN. [d] Dipping solutions were prepared at a concentration of 0.1 mM of Zn^{II}Pc and with 10 mM of CHENO in THF. V_{OC} = open circuit voltage, J_{SC} = short-circuit current density, FF = fill factor, η = solar-to-electric power conversion efficiency.

avoid Pc aggregation and to obtain optimal performances in DSSCs. As a general trend, the overall efficiency of the *para* derivatives was superior to that of the *meta* analogues, both in the mono- (1.3 vs. 0.44%) and disubstituted (0.89 vs. 0.11%) series. This low efficiency mainly results from the systematically lower J_{SC} values of the *meta* derivatives with respect to the *para* analogues. There are several possible explanations for these results. On the one hand, the *meta* substitution of the anchoring pyridyl group reduces the amount of adsorbed molecules because the dye molecules take up more space on the TiO$_2$ surface leading to suboptimal packing (Figure S10). On the other hand, the "tilted" binding modality adopted by dyes adsorbed on TiO$_2$ is also known to increase the charge-recombination rate between the oxidized dye and the injected electrons e$^-$/TiO$_2$ conduction band (CB) because of the close proximity between the macrocycle core and the surface.[14–16] Both factors could explain the poorer J_{SC} values, and hence lower power conversion efficiencies of the *meta*-type dyes relative to their *para* analogues. Another interesting trend was observed in both *meta* and *para* series: The dyes **TT52** and **TT53** anchored to the TiO$_2$ through only one pyridyl group gave systematically much higher efficiencies than their respective disubstituted analogues **TT54** and **TT55**. The exact explanation for this observation is currently not known. A similar trend was previously observed by us for some Pcs substituted with only one carboxyl anchoring group which gave either better[17] or poorer[18] performances in DSSC than the corresponding disubstituted analogues. We could speculate that in the case of **TT55** and **TT56**, the presence of two anchoring groups leads to a different arrangement of the dye on the surface which might have important consequences on the directionality and/or binding strength, ultimately affecting the electron injection process and recombination kinetics. Another possible explanation could involve changes in the electron density owing to the presence of a second acceptor/anchoring group hence affecting the MO energy levels of the Pc dyes.

Due to the high aggregation tendency of tri-*tert*-butyl Zn^{II}Pcs, a large amount of co-adsorbent is most often required to prevent the sensitizer's aggregation and reach optimal performance in DSSCs (typically, a CHENO/Pc ratio of 100:1). However, this presents a drawback since the adsorption of the co-adsorbent to the active surface reduces the dye's adsorption, which limits the J_{SC}, and hence the overall PCE efficiency. This effect is much more pronounced for the pyridyl-functionalized Pcs than for carboxyl-substituted ones, as one can appreciate by the different color of the photoanodes in Figure 2 (vide infra).

This could constitute one of the reasons for the relative low photocurrent obtained for the pyridyl-functionalized Pcs. It is important to emphasize that this issue is specific to our dyes, and was not encountered with other pyridyl-substituted sensitizers previously described in the literature, such as porphyrins, because of the much lower amount of co-adsorbent required for optimal performance, typically a CHENO/porphyrin ratio of 1:1.[1] In order to tackle this issue for pyridyl-substituted Pcs, the use of non-aggregating Pcs that require little or no addition of CHENO would certainly be a viable alternative,[2, 18] and

Figure 2. Pictures of the DSSC devices made with dyes **TT1**, **TT41**, **TT59**, **TT55** and **TT60** adsorbed on [9+4] μm thick films; dye solutions were prepared at a concentration of 0.1 mM of Pc and 10 mM of CHENO in THF (except for **TT1** in EtOH).

Figure 3. Top: pictures of the DSSC devices made with **TT55** (0.1 mM in THF) and different concentration of CHENO (0, 1, 4, and 10 mM in THF) adsorbed on [9+4] μm thick films; the benchmark device made with the carboxyl-substituted dye **TT1** (0.1 mM) in EtOH with 10 mM of CHENO is shown for comparison purpose. Bottom: Enlargement of the active area.
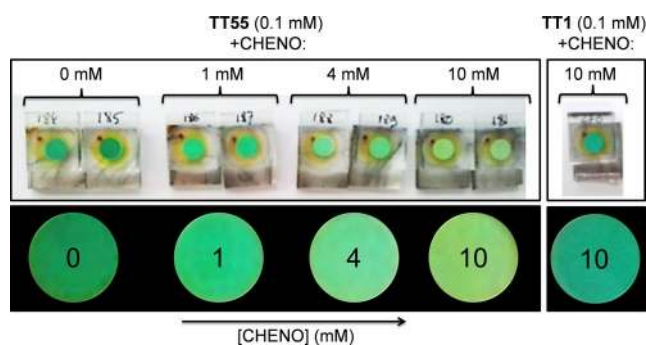
this approach is currently being examined in our groups. In order to rationalize how the ratio of Pc to co-adsorbent affects the PV performance of the resulting devices, different solutions of **TT55** in THF were prepared at a dye concentration of 0.1 mM with CHENO at 0, 1, 4, or 10 mM (Table 2). As can be appreciated in Figure 3 from the color of the photoanodes,

Table 2. Effect of co-adsorbent CHENO on the performance of the DSSC devices[a] made with **TT55** (0.1 mM in THF) adsorbed on [9+4][b] μm thick TiO$_2$ films; PV data under simulated full sun illumination (AM1.5G) using the iodine-based electrolyte A; active area of 0.159 cm^{-2}.

CHENO [mM]	Electrolyte[c,d]	V_{OC} [mV]	J_{SC} [mA cm^{-2}]	FF [%]	P_{in} [mW cm^{-2}]	η [%]
0	A	507	1.28	74.6	97.4	0.50
1	A	521	1.99	76.9	98.0	0.81
4	A	529	2.00	75.0	97.7	0.81
10	A	552	2.00	77.0	97.4	0.87

[a] Two or three devices of equal quality were made for each configuration; the values obtained for the best cell are presented in each case. [b] The TiO$_2$ films have a total thickness of 13 μm consisting of a 9 μm thick TiO$_2$ active layer and an additional 4 μm thick scattering layer. [c] Electrolyte A was composed of 0.025 M LiI, 0.6 M DMII, 0.28 M TBP, 0.04 M I$_2$, and 0.05 M GuNCSin AcCN. [d] Electrolyte B has the same composition as electrolyte A except with 0.1 M of LiI and 0.6 M of DMII.

the amount of adsorbed dye molecules decreased with increasing CHENO/Pc ratio, due to the competitive loading of the co-adsorbent on the surface. However, despite this, all PV parameters (J_{SC}, V_{OC}, FF, and η) increased significantly with increasing CHENO/Pc ratio. While J_{SC} reached the optimal value with 1 mM of CHENO (10-fold excess with respect to the Pc), and did not increase further at higher CHENO contents, the V_{OC} smoothly increased to reach the maximum value at the highest CHENO concentration (10 mM).

Next, we focused on the optimization of DSSC devices based on **TT55** and **TT56** in terms of the thickness of the active layer and the composition of the electrolyte. For **TT55**-based DSSC devices and with electrolyte A, the V_{OC} gradually decreases upon increasing the film thickness, from 587 mV for the [5+5] μm films to 566 mV for the [10+5] μm films. However, an opposite trend was observed for the J_{SC}, which increased from 1.70 to 2.36 mA cm^{-2} on going from the thinner

([5+5] μm) to the thicker ([10+5] μm) film. This increase can be explained by considering the higher amount of dye molecules that can be adsorbed on thicker films. **TT56**-based DSSC devices followed the same trends, but with performances systematically much lower than for the **TT55** devices (especially the J_{SC}) which is consistent with the superior efficiency of the *para-* over the *meta-*type derivatives (vide supra). Finally, the LiI concentration of the electrolyte was optimized for both **TT55** and **TT56** devices.[19] Electrolyte B has the same composition as A, except for a higher LiI concentration (i.e., 0.1 vs. 0.025 M). For **TT55** adsorbed on [10+5] μm thick TiO$_2$ films, the J_{SC} was increased from 2.36 to 4.14 mA cm^{-2} upon replacing electrolyte A with B, which represents a 75% improvement. At the same time, a 29 mV drop in the V_{OC} was observed. However, this decreases in the V_{OC} was largely compensated by the gain in the J_{SC} (from 2.36 to 4.14 mA cm^{-2}) leading to an overall efficiency of 1.7%. This latter value is 65% higher than that obtained with electrolyte A under the same conditions (η = 1.1%). Turning to **TT56**, the J_{SC} of the resulting DSSC device considerably increased when a LiI-rich electrolyte was used. With electrolyte B 0.26% and 0.32% of PCE was achieved for [9+4] and [10+5] μm thick films, which is almost three times higher than that of the [6+3] μm device using electrolyte A (Table 3). The improvement in the devices' performance upon increasing the LiI content suggests a low-lying LUMO level of these dyes.

Based on the results obtained with the pyridyl-substituted Pcs (vide supra), and as a logical extension of our previous work on DSSCs featuring carboxylic acid functionalized Pcs, we decided to combine these two moieties (i.e., carboxylic acid and pyridine) within the same dye. In this context, we prepared a tri-*tert*-butyl-substituted Zn^{II}Pc bearing an ethynyl picolinic acid unit (**TT59**). For comparative purpose, *para*-ethynylcarboxyphenyl **TT41** and 3-ethynylpyridyl **TT60** were also prepared in which the nitrogen and the carboxylic acid moieties of **TT59** were formally removed, respectively. Zn^{II}Pc **TT1**, a standard Pc sensitizer, was used as a benchmark. All dyes solutions were prepared in THF (except **TT1** in EtOH solution) at a concentration of 0.1 mM with 10 mM of CHENO as co-adsorbent. All devices were prepared under the same experimental

Table 3. Optimization of the DSSC devices[a] made with **TT55** and **TT56** (0.1 mM + CHENO 10 mM in THF) and PV data obtained under simulated full sun illumination (AM1.5G) and with active area of 0.159 cm^{-2}.

Dye	Film thickness [μm][b]	Electrolyte[c,d]	V_{OC} [mV]	J_{SC} [mA cm^{-2}]	FF [%]	P_{in} [mW cm^{-2}]	η [%]
TT55 + CHENO	[5+5]	A	587	1.70	77.5	99.4	0.78
	[6+3]	A	568	2.01	77.3	99.4	0.89
	[9+4]	A	552	2.00	77.0	97.4	0.87
	[10+5]	A	566	2.36	78.7	99.4	1.1
	[10+5]	B	537	4.14	75.7	98.6	1.7
TT56 + CHENO	[6+3]	A	493	0.301	74.3	96.5	0.11
	[9+4]	B	491	0.877	74.6	99.3	0.32
	[10+5]	B	461	0.744	73.8	97.1	0.26

[a] Two or three devices of equal quality were made for each configuration; the values obtained for the best cell are presented in each case. [b] The first and second values in brackets correspond to the thicknesses of the active and scattering TiO$_2$ layers, respectively. [c] Electrolyte A was composed of 0.025 M LiI, 0.6 M DMII, 0.28 M TBP, 0.04 M I$_2$, and 0.05 M GuNCS in AcCN. [d] Electrolyte B has the same composition as electrolyte A except with 0.1 M of LiI and 0.6 M of DMII.

procedures (i.e., dipping time of 16 h). The PV data obtained for the DSSC devices under same conditions using electrolyte B are summarized in Table 4. Among these three dyes, **TT60** gave the poorest performance with a PCE of 0.20 %. A possible explanation of the low performance of this dye could be the suboptimal electronic communication between the Pc and the

Table 4. PV data of the devices[a] made with **TT59**, model dyes **TT41** and **TT60**, and benchmark **TT1** on [9+4] μm[b] thick TiO$_2$ films using the iodine-based electrolyte B,[c] under simulated full sun illumination (AM1.5G) and with an active area of 0.159 cm^{-2}.

Dye/CHENO[d]	V_{OC} [mV]	J_{SC} [mA cm^{-2}]	FF [%]	P_{in} [mW cm^{-2}]	η [%]
TT1 + CHENO[22]	565	8.61	72.2	96.2	3.65
TT59 + CHENO	562	4.65	75.0	96.5	2.03
TT60 + CHENO	532	0.463	78.5	97.9	0.20
TT41 + CHENO	457	1.14	73.1	95.7	0.40

[a] Two devices of equal quality were made for each dyes; the values obtained for the best cell are presented in each case. [b] The TiO$_2$ films have a total thickness of 13 μm consisting of a 9 μm thick TiO$_2$ active layer and an additional 4 μm thick scattering layer. [c] Electrolyte B was composed of 0.1 M LiI, 0.6 M DMII, 0.28 M TBP, 0.04 M I$_2$ and 0.05 M GuNCS, in AcCN. [d] Dye-uptake solutions were composed of Pc 0.1 mM and CHENO 10 mM in THF solutions (except for **TT1** in EtOH solution).

TiO$_2$ surface mediated by the ethynyl-3-pyridyl unit. The high CHENO/Pc ratio required which, in turn, reduces the dye loading, as seen in Figure 2, probably also contributes to the low DSSC performance. Turning to **TT41**, a maximum PCE of 0.40 % on a [9+4] μm thick TiO$_2$ film was obtained (Table 4). This value, significantly lower than that for carboxyl-substituted tri-*tert*-butyl Zn^{II}Pcs containing no spacer (**TT1**, $\eta = 3.65$ %,

Table 4),[20] a *para*-phenyl spacer (**TT3**, $\eta = 2.2$ %),[21] and an ethynyl spacer (**TT22**, $\eta = 3.13$ %)[18] between the Pc and the COOH anchoring group, is in accordance with those previously reported for this compound ($\eta = 0.40$–0.57 %).[22] In the case of **TT41**, one could speculate that the presence of a terminal phenyl moiety in the anchoring/acceptor group lowers the electron-injection efficiency, thus explaining the low efficiency found for this dye. Likewise, in carboxyl-substituted Pors, it was found that a terminal phenyl in ethynyl-containing anchoring groups is crucial in mediating electron injection vs. back electron transfer.[11] To tackle these issues, we designed and studied Zn^{II}Pc **TT59**, containing both a carboxyl group for efficient adsorption onto TiO$_2$ and a pyridyl ring to improve the injection capability of the Pc through electronic effects. Interestingly, **TT59** showed indeed much better performance than **TT41** and **TT60**, thus profiting from the combined structural features. As a result, the overall PCE of **TT59** was boosted to 2.1 %, which is ten times higher than that of pyridyl-containing **TT60**, and five times higher than that of carboxyl-containing **TT41**. The main reason was the considerable increase in the J_{SC} of **TT59** by factors of 4 and 10 in comparison to **TT41** and **TT60**, respectively.

In conclusion, a series of seven tri-*tert*-butyl-substituted Zn^{II}Pcs containing pyridyl (one or two), ethynylpyridyl, ethynyl-carboxyphenyl, or picolinic acid groups have been prepared and their PV performances in DSSCs investigated. For the four pyridyl-anchored dyes, it was found that 1) the number of anchoring groups (one or two) and 2) the pyridyl substitution pattern (*meta* or *para*) have a strong influence on the DSSC performances of these Pcs. Under the same conditions, efficiencies of 1.3 % and 0.89 % were obtained for the *para*-substituted derivatives with one and two pyridyl anchoring groups, respectively. These PCEs are significantly higher than those found for the respective *meta*-substituted analogues (0.44 % and 0.11 %, respectively), mainly due to a better dye-to-semiconductor electronic injection and/or binding geometry of the former dyes with respect to the latter.

However, a common limitation of such pyridyl-functionalized Pcs is their poor adsorption onto the TiO$_2$, which ultimately hampers the PV performances of the DSSCs. In order to circumvent this problem, a Zn^{II}Pc peripherally substituted with a picolinic acid moiety was prepared and tested. On the one hand, the picolinic acid group acts as a good anchoring group through the carboxylic acid function. On the other hand, the presence of an electron-withdrawing nitrogen atom facilitates the dye's electron injection into the semiconductor's conduction band. For this latter dye, an improvement in the PV efficiency of up to 2.1 % was obtained. Although the presented values are still far from commercial applications, the "synergic" combination of pyridyl and carboxylic acid units within the same anchoring/acceptor group (i.e., a picolinic acid) is interesting from a conceptual viewpoint for the design of a new generation of Pc-based dyes for DSSCs.

[1] M. Urbani, M. Grätzel, M. K. Nazeeruddin, T. Torres, *Chem. Rev.* **2014**, *114*, 12330 – 12396.

[2] M.-E. Ragoussi, M. Ince, T. Torres, *Eur. J. Org. Chem.* **2013**, 6475 – 6489.

[3] G. Bottari, G. de la Torre, D. M. Guldi, T. Torres, *Chem. Rev.* **2010**, *110*, 6768 – 6816.

[4] T. Higashino, Y. Fujimori, K. Sugiura, Y. Tsuji, S. Ito, H. Imahori, *Angew. Chem. Int. Ed.* **2015**, *54*, 9052 – 9056; *Angew. Chem.* **2015**, *127*, 9180 – 9184.

[5] K. Ladomenou, T. N. Kitsopoulos, G. D. Sharma, A. G. Coutsolelos, *RSC Adv.* **2014**, *4*, 21379 – 21404.

[6] Y. Ooyama, S. Inoue, T. Nagano, K. Kushimoto, J. Ohshita, I. Imae, K. Komaguchi, Y. Harima, *Angew. Chem. Int. Ed.* **2011**, *50*, 7429 – 7433; *Angew. Chem.* **2011**, *123*, 7567 – 7571.

[7] J. Lu, X. Xu, Z. Li, K. Cao, J. Cui, Y. Zhang, Y. Shen, Y. Li, J. Zhu, S. Dai, W. Chen, Y. Cheng, M. Wang, *Chem. Asian J.* **2013**, *8*, 956 – 962.

[8] D. Daphnomili, G. D. Sharma, S. Biswas, K. R. Justin Thomas, A. G. Coutsolelos, *J. Photochem. Photobiol. A* **2013**, *253*, 88 – 96.

[9] D. Daphnomili, G. Landrou, S. Prakash Singh, A. Thomas, K. Yesudas, K. Bhanuprakash, G. D. Sharma, A. G. Coutsolelos, *RSC Adv.* **2012**, *2*, 12899 – 12908.

[10] T. Ikeuchi, S. Agrawal, M. Ezoe, S. Mori, M. Kimura, *Chem. Asian J.* **2015**, *10*, 2347 – 2351.

[11] C.-L. Mai, T. Moehl, C.-H. Hsieh, J.-D. Décoppet, S. M. Zakeeruddin, M. Grätzel, C.-Y. Yeh, *ACS Appl. Mater. Interfaces* **2015**, *7*, 14975 – 14982.

[12] J. H. Delcamp, A. Yella, M. K. Nazeeruddin, M. Grätzel, *Chem. Commun.* **2012**, *48*, 2295 – 2297.

[13] J.-J. Cid, J.-H. Yum, S.-R. Jang, M. K. Nazeeruddin, E. Martinez-Ferrero, E. Palomares, J. Ko, M. Grätzel, T. Torres, *Angew. Chem. Int. Ed.* **2007**, *46*, 8358 – 8362; *Angew. Chem.* **2007**, *119*, 8510 – 8514.

[14] H. Matsuzaki, T. N. Murakami, N. Masaki, A. Furube, M. Kimura, S. Mori, *J. Phys. Chem. C* **2014**, *118*, 17205 – 17212.

[15] A. S. Hart, C. B. Kc, H. B. Gobeze, L. R. Sequeira, F. D'Souza, *ACS Appl. Mater. Interfaces* **2013**, *5*, 5314 – 5323.

[16] T. Higashino, H. Imahori, *Dalton Trans.* **2015**, *44*, 448 – 463.

[17] M. García-Iglesias, J.-H. Yum, R. Humphry-Baker, S. M. Zakeeruddin, P. Pechy, P. Vázquez, E. Palomares, M. Grätzel, M. K. Nazeeruddin, T. Torres, *Chem. Sci.* **2011**, *2*, 1145 – 1150.

[18] M.-E. Ragoussi, J.-J. Cid, J.-H. Yum, G. de la Torre, D. Di Censo, M. Grätzel, M. K. Nazeeruddin, T. Torres, *Angew. Chem. Int. Ed.* **2012**, *51*, 4375 – 4378; *Angew. Chem.* **2012**, *124*, 4451 – 4454.

[19] M. Urbani, M. Medel, S. A. Kumar, M. Ince, A. N. Bhaskarwar, D. González-Rodríguez, M. Grätzel, M. K. Nazeeruddin, T. Torres, *Chem. Eur. J.* **2015**, *21*, 16252 – 16265.

[20] J. Fernández-Ariza, M. Urbani, M. Grätzel, M. S. Rodríguez-Morgade, M. K. Nazeeruddin, T. Torres, *ChemPhotoChem* **2017**, DOI: 10.1002/cptc.201600004.

[21] J.-J. Cid, M. García-Iglesias, J.-H. Yum, A. Forneli, J. Albero, E. Martínez-Ferrero, P. Vazquez, M. Grätzel, M. K. Nazeeruddin, E. Palomares, T. Torres, *Chem. Eur. J.* **2009**, *15*, 5130 – 5137.

[22] G. Zanotti, N. Angelini, A. M. Paoletti, G. Pennesi, G. Rossi, A. A. Bonapasta, G. Mattioli, A. Di Carlo, T. M. Brown, A. Lembo, A. Reale, *Dalton Trans.* **2011**, *40*, 38 – 40.